

Supporting Information for

Polyurethane Elastomers with Amphiphilic ABA *Tri*-Block Copolymers as the Soft Segments Harvesting Record-High Tensile Strength and Simultaneously Increased Ductility

Jun Ma,^a Baixue Deng,^a Yanbin Fan,^{*b} Xiayun Huang,^a Daoyong Chen,^{*a} Yan Ma,^b Hongyu Chen,^b Adam L. Grzesiak^c and Shaoguang Feng^b

^aThe State Key Laboratory of Molecular Engineering of Polymers and Department of Macromolecular Science, Fudan University, 2005 Songhu Road, Shanghai 200438, China. E-mail: chendy@fudan.edu.cn

^bThe Dow Chemical Company, 936 Zhangheng Road, Shanghai 201203, China. E-mail: yfan11@dow.com

^cThe Dow Chemical Company, 693 Washington Street, Midland, Michigan 48640, United States

Table of Contents

2. Experiments.....	3
2.1 Synthesis of the <i>tri</i> -Block Co-Polymer Diols.....	3
2.2 Synthesis of the Prepolymers and Polyurethanes.....	4
3. Characterization Methods	5
3.1 Nuclear Magnetic Resonance Spectroscopy (NMR).....	5
3.2 Gel Permeation Chromatography (GPC).....	6
3.3 Attenuated Total internal Reflection Infrared Spectroscopy (ATR-IR).....	7
3.4 Atomic Force Microscopy (AFM).....	8
3.5 Dynamic Simulations	9
3.6 Tensile Experiments	10
3.7 Recoverability Experiments.....	11
3.8 Scanning Electron Microscopy (SEM).....	11
3.9 Dynamic Mechanical Analysis (DMA).....	12
3.10 Differential Scanning Calorimetry (DSC).....	12
3.11 Synchrotron Radiation Small-Angle X-ray Scattering (SAXS) and Wide-Angle X-ray Scattering (WAXS)	13
4. References	14

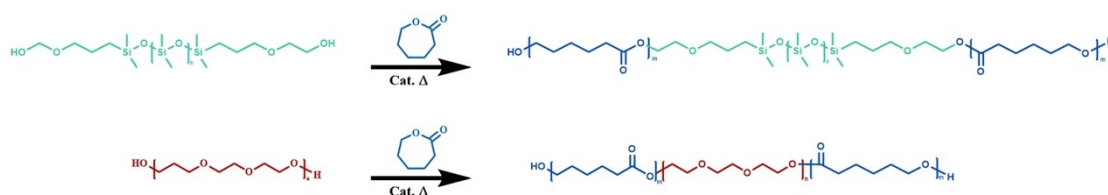
1. Materials

Polyethylene glycols (OH-PEG-OH, $M_n \approx 1050$ and 1980 , PDI = 1.09 and 1.05 , respectively) were purchased from Alfa Aesar Co., Ltd. ϵ -Caprolactone ($\geq 99.9\%$) and Poly(ϵ -caprolactone) diol (HO-PCL-OH, $M_n \approx 2020$, PDI = 1.32) were purchased from Ju Ren Co., Ltd. Poly(dimethyl siloxane) diols (HO-PDMS-OH, $M_n \approx 1020$ and 1950 , PDI = 1.25 and 1.21) were purchased from Tanguitech Co., Ltd. 4,4'-Diphenylmethane Di-isocyanate (MDI, $\geq 99.8\%$) was purchased from BASF Co., Ltd. 1,4-Butane diol (BDO, $\geq 99.9\%$) and *n*-butyl titanate (TBT, $\geq 99.5\%$) were purchased from Aladdin Co., Ltd. Benzoyl Chloride ($\geq 99.5\%$) was purchased from Adamas Co., Ltd.

2. Experiments

2.1 Synthesis of the *tri*-Block Co-Polymer Diols

HO-PCL-PEG-PCL-OH and HO-PCL-PDMS-PCL-OH were synthesized *via* ring-opening polymerization of ϵ -caprolactone using HO-PEG-OH ($M_n \approx 1050$, PDI = 1.09) and HO-PDMS-OH ($M_n \approx 1020$, PDI = 1.25) as the macromolecular initiators, respectively. Specifically, the macromolecular initiator ($50 \text{ wt.}\%$), ϵ -caprolactone ($50 \text{ wt.}\%$) and additional *n*-butyl titanate (TBT, 25 ppm) were fed into a glass reactor equipped with a vacuum pump and oil bath under nitrogen atmosphere at room temperature. With stirring, the system was allowed to react at $120 \text{ }^\circ\text{C}$ for 17 h , followed by application of vacuum under 150 mbar and $135 \text{ }^\circ\text{C}$ for 3 h . The final product was cooled down to $80 \text{ }^\circ\text{C}$, filtered, packaged and sampled for determination.

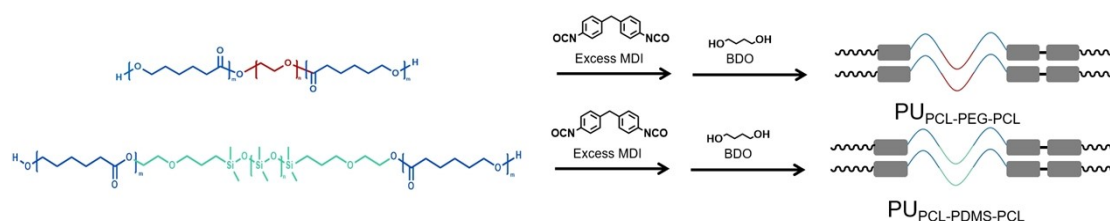


Scheme S1 Schematic illustration for the synthesis of the *tri*-block co-polymer diols

HO-PCL-PEG-PCL-OH and HO-PCL-PDMS-PCL-OH.

2.2 Synthesis of the Prepolymers and Polyurethanes

The prepolymers were synthesized by reacting the various macropolyols (soft segments) with MDI to a theoretical NCO content of 16.75 wt.% of the final products. Specifically, 55.4 wt.% of MDI and 0.1 wt.% of benzoyl chloride were fed into a 500-mL three-necked round bottom flask and mixed at 55 °C under nitrogen atmosphere. After that, 44.5 wt.% of the different macropolyols (soft segments) were charged into the flask and incubated at 85 °C for 2 hours to obtain the prepolymers, respectively. The prepolymers were then cooled to 60 °C for packaging, sampling and characterization.



Scheme S2 Schematic illustration for the synthesis of PU_{PCL-PEG-PCL} and PU_{PCL-PDMS-PCL}.

As shown in Scheme S2, polyurethanes based on the different soft segments were then prepared *via* the following hand-mixing procedures. (a) Preheat the prepolymers and the corresponding macropolyols at 80 °C for at least 30 min to ensure low viscosity and easily mixable liquids are achieved before use. (b) Preheat the aluminum moulds with releasing agent at 110 °C for at least 30 min before the use. (c) Blend 60.8 wt.% of the prepolymers, 30.2 wt.% of the corresponding macropolyols and 9.0 wt.% of BDO (stored at room temperature) with a Flacktec. speedmixer at 2500 rpm for 1 min to efficiently mix the components and remove any air bubbles or dissolved gas. (d) Pour the mixture into the preheated moulds and keep the system at 110 °C for 1 h, followed by cooling to below 60 °C. (e) De-mold the polyurethane samples carefully to avoid damage to the samples with gloves and then post-cure the

polyurethane samples at 110 °C for at least 16 h before testing.

3. Characterization Methods

3.1 Nuclear Magnetic Resonance Spectroscopy (NMR)

High resolution ^1H -NMR spectra of HO-PCL-PEG-PCL-OH or HO-PCL-PDMS-PCL-OH were recorded using a Bruker 400 MHz spectrometer, respectively. The samples were dissolved in deuterated chloroform (CDCl_3) at a concentration of up to 10 wt.%. Chemical shifts were measured with respect to tetramethylsilane (TMS) as the internal standard.

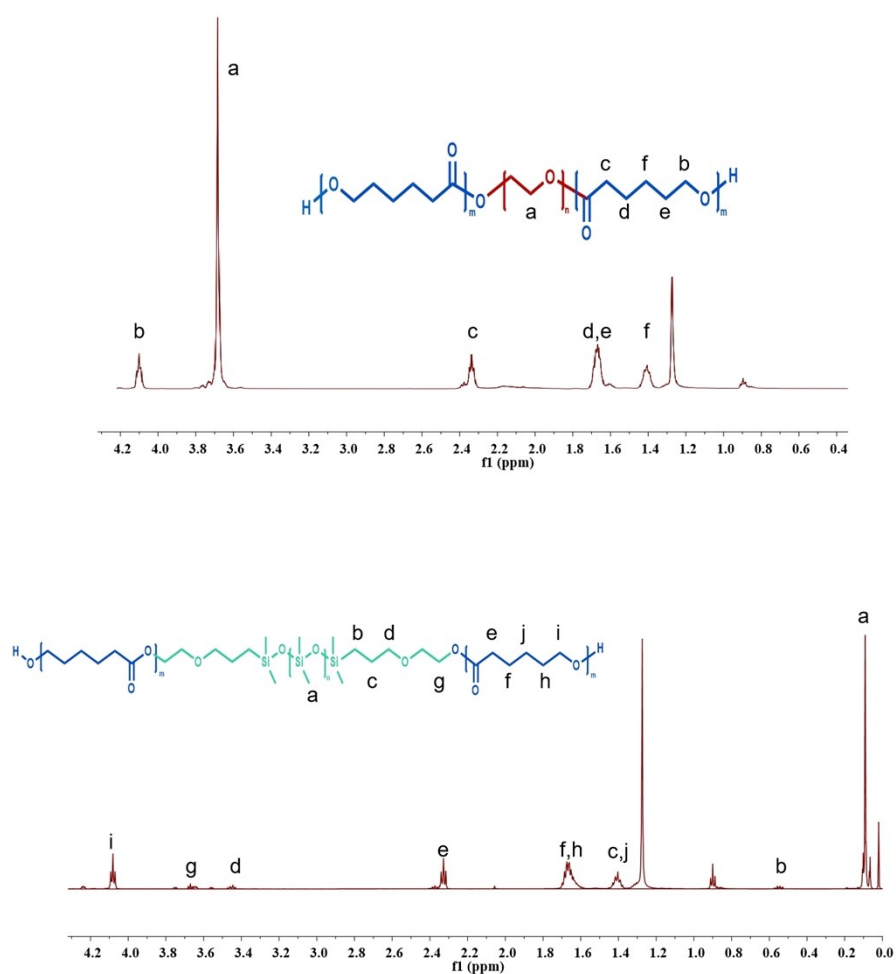


Fig. S1 ^1H -NMR spectra of the *tri*-block co-polymer diols of HO-PCL-PEG-PCL and HO-PCL-PDMS-PCL-OH in CDCl_3 at room temperature.

3.2 Gel Permeation Chromatography (GPC)

GPC (Agilent/Wyatt 1260) was used to determine the molecular weights (M_w) and PDI of the polyurethanes at 30 °C. Anhydrous N,N-Dimethylformamide (DMF) for HO-PEG-OH and HO-PCL-PEG-PCL-OH, anhydrous Tetrahydrofuran (THF) for HO-PDMS-OH and HO-PCL-PDMS-PCL-OH were used as the elution phase at a flow rate of 1.0 mL/min, respectively. Narrow polyethylene oxide standards with molecular weights ranging from 550 to 100,000 g/mol were used to calibrate the system.

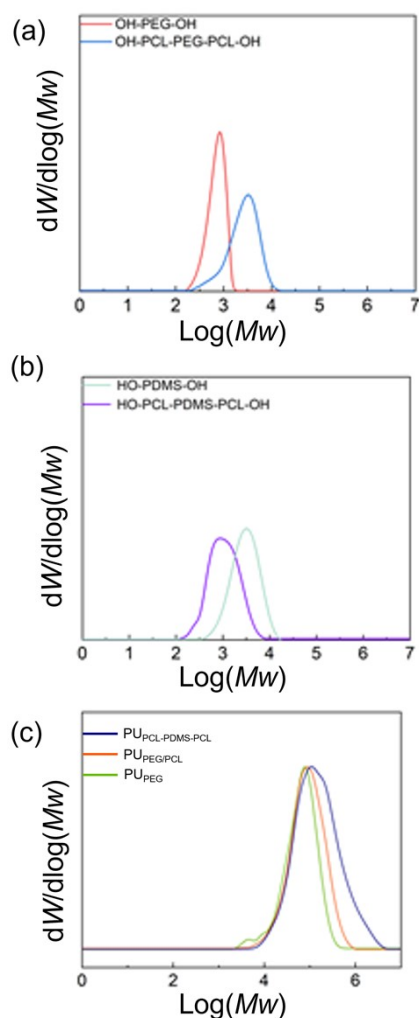


Fig. S2 GPC charts of the macromolecular initiators and the corresponding *tri*-block co-polymer diols in DMF (a) or THF (b) and GPC charts of PU_{PDMS} ($M_w = 124$ kDa, PDI = 2.86), $PU_{PDMS/PCL}$ ($M_w = 123$ kDa, PDI = 3.05) and $PU_{PCL-PDMS-PCL}$ ($M_w =$

120 kDal, PDI = 2.26) with DMF as the fluent media at room temperature.

3.3 Attenuated Total internal Reflection Infrared Spectroscopy (ATR-IR)

The polyurethanes were characterized by ATR-IR (Thermofisher Nicolet 6700) with a KRS-5 crystal of refractive index 2.4 and using an incidence angle of 45°. The resolution was 2.0 cm⁻¹ and the number of scans was 64. The results were summarized in Fig. 1b and Fig. S3.

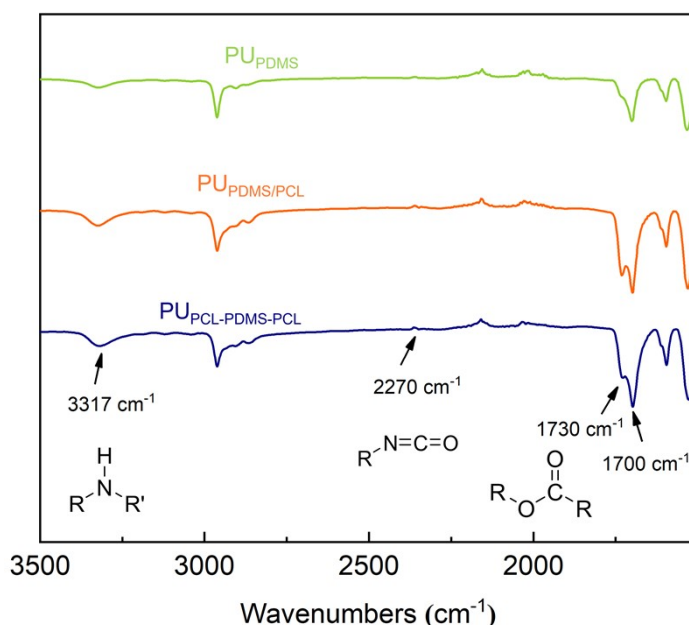


Fig. S3 The ATR-IR spectra of the synthesized polyurethanes with PDMS, PDMS/PCL mixture and PCL-PDMS-PCL *tri*-block co-polymer diols as the soft segments and MDI-BDO as the hard segments.

In the ATR-IR spectra, non-hydrogen-bonded (free) carbonyl groups appear at 1732 - 1760 cm⁻¹ (Band I), hydrogen-bonded carbonyl groups in disordered conformations appears at 1707 - 1750 cm⁻¹ (Band II), hydrogen-bonded carbonyl groups in ordered hard domains can be observed at 1665 - 1735 cm⁻¹ (Band III) and hydrogen-bonded carbonyl groups in polyester polyol in ordered soft domains appears at 1655-1690 cm⁻¹ (Band IV).¹ The different bands in the ATR-IR spectra were assigned and the area percentages (area%) of the corresponding bands were calculated

and summarized in Table S1.

Table S1. The calculated area percentages (area%) of the corresponding bands in the ATR-IR spectra for each of the polyurethanes.

	Band I (% area ~1730cm ⁻¹)	Band II (% area ~1716cm ⁻¹)	Band III (% area ~1685cm ⁻¹)	Band IV (% area ~1650cm ⁻¹)
PU_{PEG}	3.6	26.2	68.1	2.1
PU_{PEG/PCL}	2.2	27.8	63.4	6.6
PU_{PCL-PEG-PCL}	1.8	38.0	55.1	5.1
PU_{PDMS}	5.2	18.9	75.9	-
PU_{PDMS/PCL}	4.7	22.6	56.5	16.2
PU_{PCL-PDMS-PCL}	4.3	32.4	54.1	5.1

3.4 Atomic Force Microscopy (AFM)

Atomic force microscopy (AFM) was applied for characterizing the phase behaviors and morphologies of the polyurethanes. Ultrathin cross-sections of the polyurethanes were prepared using cryo-ultramicrotomy (Leica FC7-UC7), followed by the AFM characterizations on a Fastscan AFM from Bruker AXS under tapping mode. The AFM images were recorded using RTESPA-150 silicon cantilevers ($k = 5 \text{ N}\cdot\text{m}^{-1}$). To compare the AFM phase contrast images in a semi-quantitative way, software ImageJ and a bandpass filter were applied to process and smooth the images, respectively. After that, a brightness threshold was used for highlighting areas representative of the hard domains. All surrounding areas were masked to obtain a maximal contrast (Fig. S4). The distribution of average Feret diameters was then obtained from the fitted domains in each image.

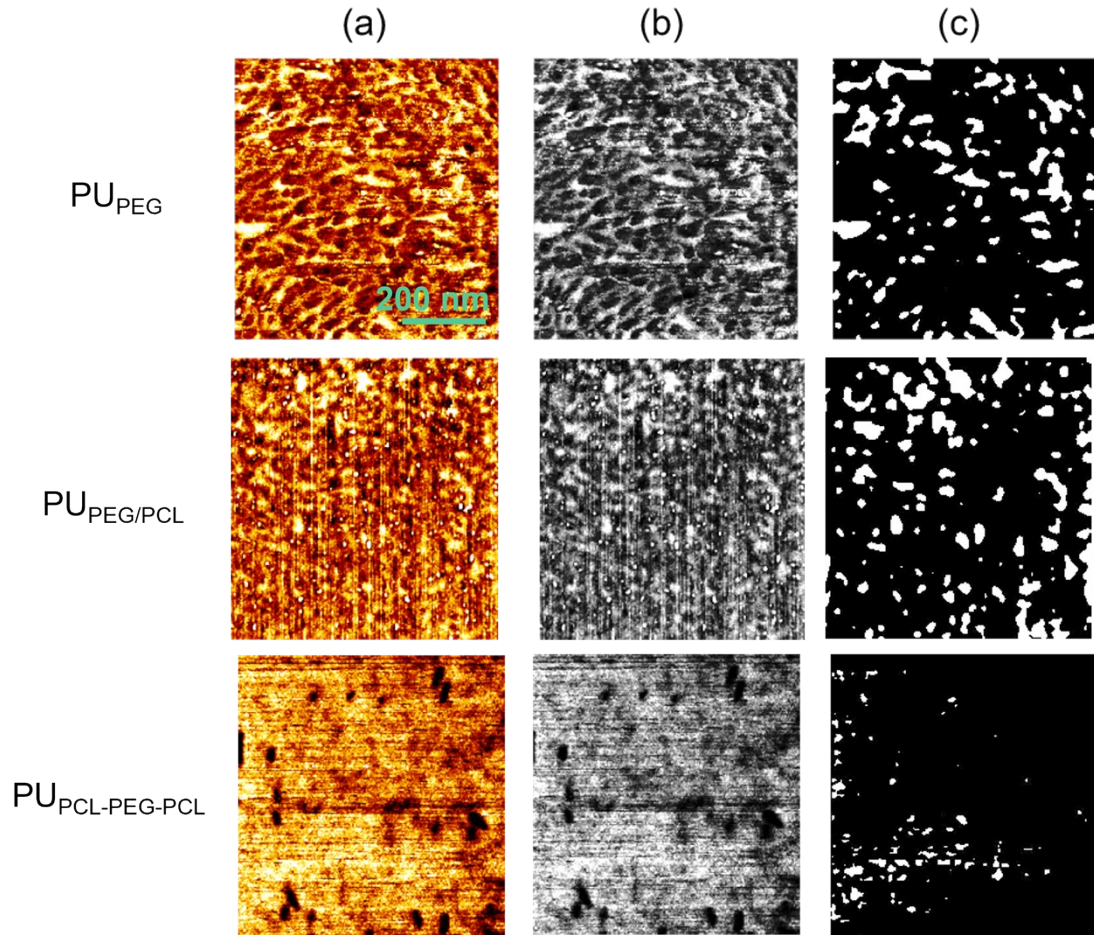


Fig. S4 (a) Original, (b) processed and smoothed and (c) hard-domain highlighted AFM images for PU_{PEG} , $PU_{PEG/PCL}$ and $PU_{PCL-PEG-PCL}$.

3.5 Dynamic Simulations

The mesoscopic simulations were conducted based on the MesoDyn Module in BIOVIA Materials Studio® environment. The simulations were performed at 298 K with a grid dimension of $32 \times 32 \times 32 \text{ nm}^3$, where the grid spacing was 1.0 nm and the bond length was 1.1543 nm. The bead diffusion coefficient and noise parameter were set to be $1.0 \cdot e^{-7} \text{ cm}^2/\text{s}$ and 75.002, respectively. The simulation time for each step was 50 ns and the total steps for each simulation were 100 steps. The method of processing the simulations model images via software ImageJ was the same as the way described in the Section 3.4.

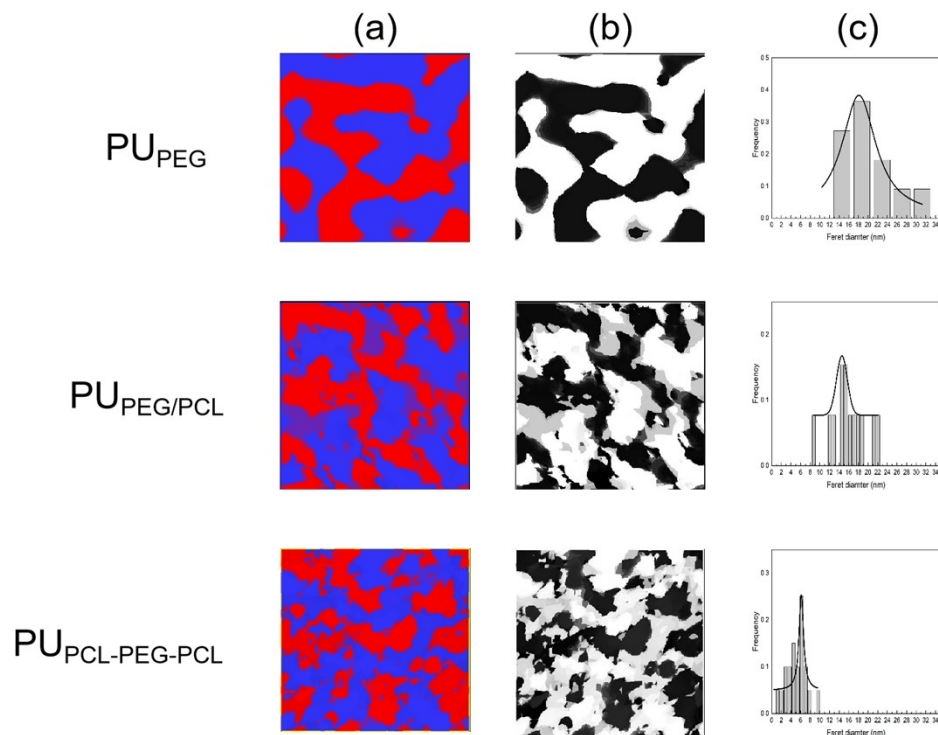


Fig. S5 (a) Original, (b) processed and smoothed highlighted simulations model images for PU_{PEG} , $PU_{PEG/PCL}$ and $PU_{PCL-PEG-PCL}$, (c) statistical size of hard domains for PU_{PEG} (20.29 nm), $PU_{PEG/PCL}$ (14.54 nm) and $PU_{PCL-PEG-PCL}$ (6.21 nm).

3.6 Tensile Experiments

Specimens ($1 \times 2 \times 12$ mm, $n = 5$) of each polyurethane were prepared and stretched to failure at a rate of 10 mm/min using an Instron 5966 uniaxial tensile tester equipped with a 1 kN load cell. The elastic modulus, tensile strength, and ultimate elongation at break were calculated from the resultant engineering stress/strain curves. A secant modulus based on 2% strain was calculated for the elastic modulus and subsequently referred to as the modulus.

Table S2. Summary of the tensile stress and elongation at break for each of the polyurethanes ($n = 5$).

	Tensile stress (MPa)	Elongation at break (%)
$PU_{PCL-PEG-PCL}$	71 ± 6	627 ± 21

PU _{PEG/PCL}	33±2	489±23
PU _{PEG}	10±1	529±22
PU _{PDMS}	6±1	33±5
PU _{PCL-PDMS-PCL}	27±1	466±10
PU _{PDMS/PCL}	14±2	157±13

3.7 Recoverability Experiments

For the recovery rate test, the specimens (1×2×12 mm) with original length of L_0 were stretched to a 250% stress strain, followed by the measurements of the sample length (L_t) after 24 h and 36 h post-stretching at room temperature, respectively (Fig. S5). Then recovery rate for each of the samples was calculated according to the following equation:

$$\text{recovery rate} = (2.5 \cdot L_0 - L_t) / (2.5 \cdot L_0 - L_0) \cdot 100\%$$

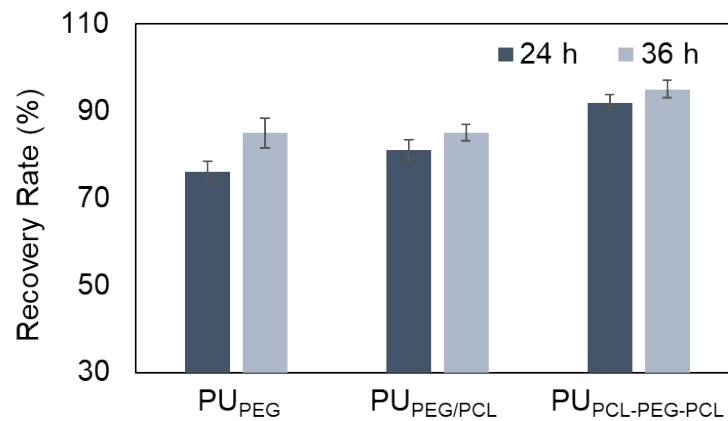


Fig. S6 Recovery rates of PU_{PEG}, PU_{PEG/PCL} and PU_{PCL-PEG-PCL} after 24 h or 36 h post-stretching to 250% tensile strain, respectively.

3.8 Scanning Electron Microscopy (SEM)

The surface morphology of the tensile fractures was examined with a field emission scanning electron microscope (FESEM, Zeiss Ultra 55 model) instrument

operated at 5 KV. The fractured side of each sample was placed vertically in the sample holder and gold-coated before microscopy with the FESEM.

3.9 Dynamic Mechanical Analysis (DMA)

The dynamic mechanical properties of the polyurethanes were evaluated by DMA (TAQ800) in three points bending geometry mode, using a static strain of $\sim 0.05\%$. The temperature was varied from -100 to 200 °C with a scanning rate of 5 °C/min and constant operation frequency of 1 Hz. Dimensions of the samples were approximately 22 mm \times 5 mm \times 1 mm (length \times width \times thickness).

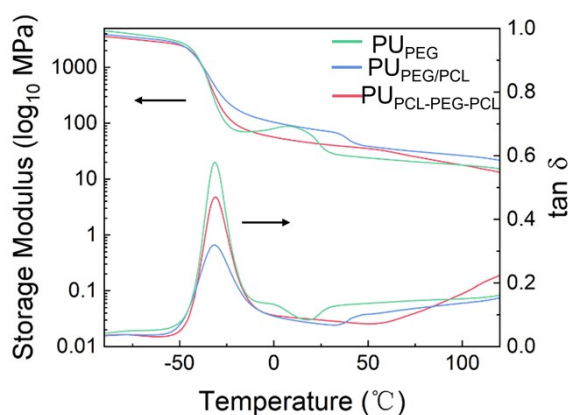


Fig. S7 DMA charts with storage modulus and $\tan\delta$ versus temperature of the polyurethanes of PU_{PEG}, PU_{PEG/PCL} and PU_{PCL-PEG-PCL}.

3.10 Differential Scanning Calorimetry (DSC)

DSC measurements were carried out in a TA Q2000 equipment, provided with an electric intracooler as a refrigerator unit. Three samples with a weight between 5 and 10 mg each were held in aluminum pans and heated from 40 to 220 °C at a scanning rate of 20 °C/min under a constant nitrogen flow to eliminate heat history and then cool down to -70 °C at the same scanning rate. Finally, these samples were heated to 220 °C at a scanning rate of 5 °C/min under a constant nitrogen flow. In the 2nd round heating curves, crystallizing (T_c) or melting temperatures (T_m) was settled

as the maximum of exothermic peak or minimum of endothermic peak.

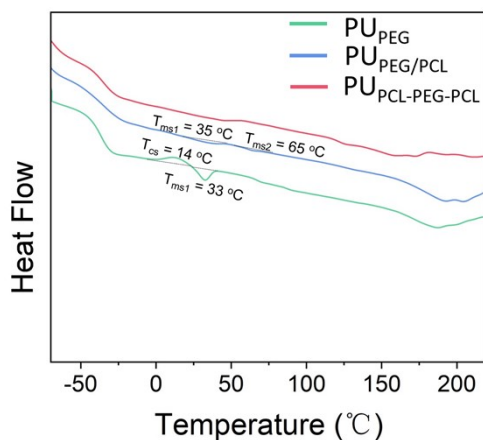


Fig. S8 DSC charts of the 2nd round heating curves of PU_{PEG}, PU_{PEG/PCL} and PU_{PCL-PEG-PCL}.

3.11 Synchrotron Radiation Small-Angle X-ray Scattering (SAXS) and Wide-Angle X-ray Scattering (WAXS)

In-situ SAXS and WAXS measurements were performed in the beamline BL16B1 at Shanghai Synchrotron Radiation Facility (SSRF). The radiation wavelength was 0.156 nm. The distance from the sample to the detector at BL16B1 for SAXS and WAXS measurements was set to be 1920 mm and 112.1mm, respectively. The distance was calibrated using silver behenate. In the beamline, a MARCCD 165 detector (Mar research, Norderstedt, Germany) binned by 1475 × 1679 was employed to record the 2D data. All the SAXS and WAXS patterns were recorded continuously upon the continuous drawing of the samples. The cycle time was 20 s in the SAXS and WAXS measurement. The sample was well-adjusted to be perpendicular to the X-ray beam.

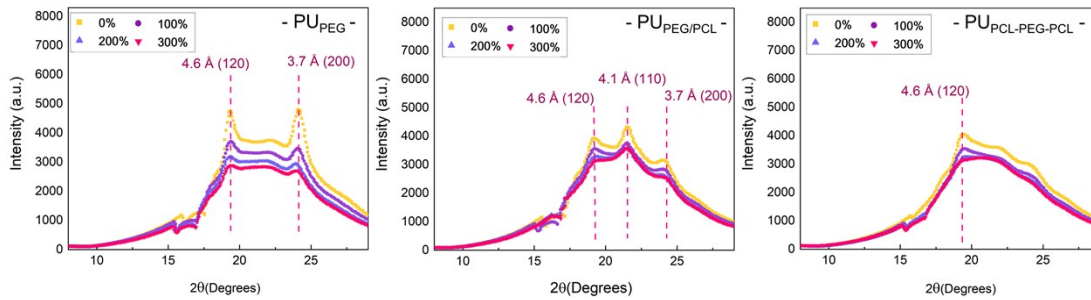


Fig. S9 1D-WAXD profiles on the meridian direction for different polyurethanes at 0%, 100%, 200% and 300% strain.

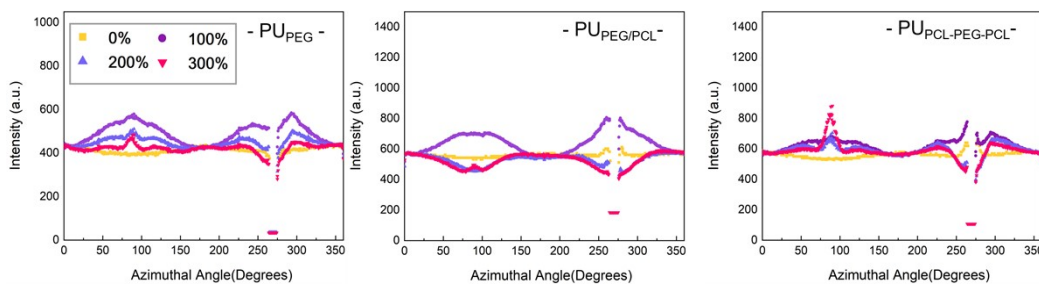


Fig. S10 Azimuthal profiles of the 2D-SAXS patterns at $q = 0.2 - 0.6 \text{ nm}^{-1}$ of the polyurethanes at 0%, 100%, 200% and 300% strains.

4. References

1. L. Rueda-Larraz, B. F. d'Arilas, A. Tercjak, A. Ribes, I. Mondragon, A. Eceiza, *Eur. Polym. J.*, 2009, **45**, 2096-2109.